Copyright © 2006 by the Genetics Society of America
DOI: 10.1534/genetics.106.056762

Characterization of Drosophila *mini-me*, a Gene Required for Cell Proliferation and Survival

Chonnettia Jones,* Rita Reifegerste*,† and Kevin Moses*,‡,[1]

**Department of Cell Biology, Emory University School of Medicine, Atlanta, Georgia 30322,* †*Evotec Neurosciences GmbH, Hamburg, Germany and* ‡*Howard Hughes Medical Institute, Janelia Farm Research Campus, Ashburn, Virginia 20147*

Manuscript received February 6, 2006
Accepted for publication March 16, 2006

ABSTRACT

In the developing Drosophila eye, the morphogenetic furrow is a developmental organizing center for patterning and cell proliferation. The furrow acts both to limit eye size and to coordinate the number of cells to the number of facets. Here we report the molecular and functional characterization of Drosophila *mini-me* (*mnm*), a potential regulator of cell proliferation and survival in the developing eye. We first identified *mnm* as a dominant modifier of *hedgehog* loss-of-function in the developing eye. We report that *mnm* encodes a conserved protein with zinc knuckle and RING finger domains. We show that *mnm* is dispensable for patterning of the eye disc, but required in the eye for normal cell proliferation and survival. We also show that *mnm* null mutant cells exhibit altered cell cycle profiles and contain excess nucleic acid. Moreover, *mnm* overexpression can induce cells to proliferate and incorporate BrdU. Thus, our data implicate *mnm* as a regulator of mitotic progression during the proliferative phase of eye development, possibly through the control of nucleic acid metabolism.

CELL proliferation and growth in the developing Drosophila compound eye are regulated in two distinct phases, separated by the morphogenetic furrow (Thomas *et al.* 1994; Ready *et al.* 1976; Baker 2001). During embryogenesis, ~20 cells are set aside to form the eye imaginal disc and grow by unpatterned proliferation. In the third instar, a wave of differentiation and patterning called the morphogenetic furrow passes across the eye field from posterior to anterior (Ready *et al.* 1976). In the furrow, cells are held in G1 arrest and a process of Delta/Notch-mediated lateral inhibition initiates pattern formation by specifying ommatidial founder cells (the future R8 photoreceptors, Baker 2001; Frankfort and Mardon 2002). Posterior to the furrow, cells surrounding the R8 are recruited to specific fates by successive rounds of Ras pathway signaling, modulated by further Notch-mediated signals (Nagaraj and Banerjee 2004; Voas and Rebay 2004).

The first five ommatidial cells remain in G1 arrest posterior to the furrow, but the surrounding cells reenter the cell cycle for one more round of cell division, the "second mitotic wave." The remaining 15 ommatidial cells are derived from the daughters of this division (Ready *et al.* 1976; Tomlinson 1988; Baker 2001). Later, in pupal life, excess cells are removed by programmed cell death (Cagan and Ready 1989; Wolff and Ready 1991; Baker 2001) and the end result is a precisely constructed eye with 20 cells per facet. The regulation of cell cycle progression in the second mitotic wave has been shown to depend on Egfr, Notch, Hedgehog, and Decapentaplegic signaling, acting through Cyclins A and E, as well as on RBF, E2F, and Dacapo (de Nooij *et al.* 1996, 2000; Baker and Yu 2001; Duman-Scheel *et al.* 2002; Tseng and Hariharan 2002; Baonza and Freeman 2005; Firth and Baker 2005).

Thus, in normal development the different ommatidial cell types are derived from two different proliferative generations. However, this generational difference is not required. When the second mitotic wave is abolished (by the ectopic expression of a cyclin kinase inhibitor), all the retinal cells are derived from cell divisions that occur anterior to the furrow (de Nooij and Hariharan 1995). Under these circumstances, the eye lacks sufficient cells and some terminal fates are left unfilled; yet, most cells differentiate normally.

The morphogenetic furrow acts both to limit eye size (by ending the first mitotic wave) and to coordinate the number of cells to the number of facets (the second mitotic wave). The key regulator of the furrow is Hedgehog, which is expressed posterior to the furrow and activates downstream genes anterior to the furrow, via the regulation of Smoothened and Patched (Heberlein and Moses 1995; Lum and Beachy 2004). In addition, Hedgehog induces Decapentaplegic expression in the furrow (Heberlein and Moses 1995). Decapentaplegic is thought to act redundantly with Hedgehog anterior to the furrow (Greenwood and Struhl 1999; Fu and Baker 2003) and independently of Hedgehog at the margins of the disc (Pignoni and Zipursky 1997). Some genetic regulators of the cell cycle differ in the first and

[1]*Corresponding author:* Howard Hughes Medical Institute, Janelia Farm Research Campus, 19710 Janelia Farm Blvd., Ashburn, VA 20147. E-mail: mosesk@hhmi.org

second mitotic waves. For example, mosaic clones lacking the Hedgehog receptor Smoothened are as large as their wild-type twin spots anterior to the furrow (Strutt and Mlodzik 1996) but do not synthesize DNA in the second mitotic wave (Duman-Scheel *et al.* 2002). In contrast, the size of *Egfr* clones (and other Ras pathway gene clones) is stunted on both sides of the furrow (Xu and Rubin 1993).

Hedgehog signaling has been implicated as a direct regulator of cell proliferation in the developing eye disc and the Hedgehog pathway element *patched* was recovered in a screen for genes that interact with *RBF* (Duman-Scheel *et al.* 2002). Hedgehog can regulate the transcription of Cyclins E and D, and ectopic Hedgehog signaling can activate Cyclin E reporter expression in the furrow (Duman-Scheel *et al.* 2002). Hedgehog also may act redundantly with Decapentaplegic to regulate G1 cell cycle arrest in the furrow (Penton *et al.* 1997; Horsfield *et al.* 1998; Duman-Scheel *et al.* 2002; Firth and Baker 2005). Cells lacking the Hedgehog pathway transcription factor gene *cubitus interruptus* (*ci*) arrest prematurely in G1 (Firth and Baker 2005). Furthermore, Ci overexpression in the furrow causes cells normally arrested in G1 to enter S-phase and incorporate Bromo-deoxy Uridine (BrdU) (Duman-Scheel *et al.* 2002). Also, cells that are doubly mutant for Hedgehog and Decapentaplegic pathway signaling show the strongest effects on G1 arrest by retaining Cyclin B expression and BrdU incorporation (Firth and Baker 2005).

Here we report the identification and genetic, molecular, and phenotypic characterization of a Drosophila gene, *mini-me* (*mnm*). We first identified an allele of *mnm* as a dominant modifier of *hedgehog* loss-of-function. We find that *mnm* encodes a conserved protein and that *mnm* transcription is regulated by Hedgehog signaling, on both sides of the furrow. *mnm* is required for normal cell proliferation and for cell survival anterior to the furrow, but not posterior to it. Mnm appears to function in the regulation of cell nucleic acid metabolism. Thus *mnm* may provide new insight into the control of cell proliferation and survival in the developing eye disc.

MATERIALS AND METHODS

Drosophila stocks, mutagenesis screen, and germline excision: Wild-type stocks were w^{1118} and ry^{506}. For the screen, autosomally isogenic w^{1118}; cn^1; e^s P((*w*, *ry*)D)3 hh^{bar3} males were treated with 25 mm EMS and crossed to autosomally isogenic w^{1118}; hh^8/*TM6B* females. Mutations were recovered from the F_1 male progeny. For the excision screen, p(ry^+(t7.2) = Delta2–3)99B (Laski and Rubin 1989) was used to mobilize the p(PZ) element in *l(2)rQ313*. Five hundred thirty $rosy^-$ lines were tested by genomic DNA gel blot (probe, transgene 2, Figure 2A). mnm^{PX1} deletes 1488 bp rightward from *l(2)rQ313*, removing the translation start site and three conserved protein domains (N-terminal, Zn knuckle, and RING). Three precise excision revertant alleles restored viability, confirming that the lethality associated with the *l(2)rQ313* chromosome was solely due to the *P*-element insertion in *mnm*.

Mutant/transgenic stocks:

w^{1118}; hh^{ts2}/TM6B
hh:GAL4/TM6B and *hh:GAL4 UAS:GFP*/TM6B (gifts from T. Tabata)
en:GAL4 (gift from Ruth Palmer)

From the Bloomington Stock Center:

l(2)rQ313^{rQ313}/CyO
w^{1118}; *P(ry*$^+$*=neoFRT)42D* P(w^{+mC}=*Ubi:GFP.nls*)2R1 P(*Ubi:GFP.nls*)2R2
w^{1118}; *P(ry*$^+$*=neoFRT)42D*
w^{1118}; *P(ry*$^+$*=neoFRT)42D P(w*$^+$*,ry*$^+$*)47A*
w^{1118}/GMR:p35
sp/CyO; UAS-*P35*/TM6B
ey:FLP (Newsome *et al.* 2000)
hs:FLP (Xu and Rubin 1993)

Phage library screen, DNA constructs, and transgenic lines:

Library: 17–23 kb, *Sau*3a partially digested, genomic DNA from the autosomally isogenic screen parent line was inserted into the *Xho*I site of λFIX (Stratagene, La Jolla, CA).

Probe: PCR fragment flanking the *l(2)rQ313* site [Roche (Indianapolis) High Prime DNA-labeling kit]. Thirty-nine unique phage isolates and transgenic constructs were confirmed by restriction mapping and end sequencing. Germline transformations were performed as previously described (Rubin and Spradling 1982).

Transgene 1: 8023-bp *Xba*I genomic fragment (2308 bp left of *mnm* transcript to 331 bp after the 3′ end) in pCaSpeR-4 (Thummel and Pirotta 1992).

Transgene 2: 14,701-bp *Eag*I genomic fragment in the *Not*I site of pCaSpeR-3 (Thummel and Pirotta 1992).

Transgene 3: From transgene 2 by *Acc*65I digest and then Klenow fill-in to disrupt the splice acceptor site at the start of exon 4 for a frameshift at residue 135.

Transgene 4: From transgene 2 by *Spe*I digest and religation to produce a 2888-bp deletion, eliminating *mnm* exons 7–9, and terminating the protein after residue 491. Tests of rescue were for adult viability of all homozygous and *trans*-heterozygous combinations of mnm^1, mnm^P, and mnm^{PX1}.

mnm overexpression construct: cDNA LD21643 (3937 bp; Research Genetics, Birmingham, AL) between the *Not*I and *Xho*I of pUAST (Brand and Perrimon 1993). Germline transformations were performed as described above. *mnm* overexpression was driven by *en:GAL4* and flies were raised at 18°, 25°, or 29°. Ten transgenic lines that were obtained exhibited similar phenotypes.

Gel blots: Poly(A)$^+$ RNA from w^{1118} embryos, larvae, and adults was analyzed by gel blot (Sambrook *et al.* 1989). The probe was ^{32}P-labeled cDNA LD21643 (Roche High Prime DNA-labeling kit).

RT–PCR: Single *mnm* heterozygote or mutant embryos were identified using GFP balancer chromosomes and confirmed by PCR. RNA was isolated from single embryos [QIAGEN (Valencia, CA) RNeasy kit]. The RNA preparation contained contaminating genomic DNA, which was included as a loading control. The RT–PCR reactions were performed according to the QIAGEN One-Step RT–PCR protocol. RT–PCR products were resolved by agarose gel electrophoresis. The primers used to detect the *mnm* transcript were primers that amplified a portion of exons 8 and 9. *mnm* primer sequences were 5′-GCTGCTTTGTGATGCTTCCG-3′ and 5′-CAACTCCAGGGATAATCTCAAGGAC-3′.

Microscopy, *in situ* hybridization, and immunohistochemistry: Scanning electron microscopy was performed as previously described (Tio and Moses 1997). The statistical analyses of ommatidium numbers were by paired Student's *t*-tests. Facet counts were (a) $hh^{8}/+$, $n = 3$, mean = 674.67, SD = 32.52; (b) hh^{bar3}, $n = 4$, mean = 228.25, SD = 27.68; (c) hh^{8}/hh^{bar3}, $n = 6$, mean = 316.67, SD = 8.59; (d) $mnm^{1}/+;hh^{8}/hh^{bar3}$, $n = 6$, mean = 241.33, SD = 20.19; (e) $mnm^{P}/+;hh^{8}/hh^{bar3}$, $n = 9$, mean = 274.33, SD = 21.44; and (f) $mnm^{PX1}/+;hh^{8}/hh^{bar3}$, $n = 4$, mean = 195.25, SD = 13.60. Adult eye sections were prepared as previously described (Tomlinson 1985). Whole-mount *in situ* hybridizations were performed as previously described (Wolff 2000). The probes for the *in situ* hybridization were single-stranded digoxygenin (DIG)-labeled DNA by PCR from cDNA LD21643 and *glass* cDNA 5A6 (Roche PCR DIG probe synthesis kit; Moses *et al.* 1989). Eye disc immunohistochemistry was performed as previously described (Kumar *et al.* 1998). BrdU was performed as described (Tapon *et al.* 2001). F-actin was detected with Rhodamine-phalloidin [1:50; Molecular Probes (Eugene, OR) A-12380]. DNA was stained with Hoechst 33342 for fluorescence-activated cell sorting (FACS) (1:500; Sigma, St. Louis). The primary antisera used were rabbit anti-Ato (1:1000; Jarman *et al.* 1993), mouse anti-BrdU (1:100; BD Biosciences 33281A), mouse anti-Cyclin E (1:5, gift of B. Edgar; Richardson *et al.* 1995), rabbit activated Caspase-3 (1:200; BD Biosciences 551150; Srinivasan *et al.* 1998), rat anti-Elav (1:500, 7E8A10 from Developmental Studies Hybridoma Bank (DSHB); O'Neill *et al.* 1994), mouse anti-BarH1 (1:10, gift of K. Saigu; Higashijima *et al.* 1992), mouse anti-Cut (1:10, mAb 2B10 from DSHB; Blochinger *et al.* 1990), guinea-pig anti-Senseless (1:1000, gift of G. Mardon; Frankfort *et al.* 2001), mouse anti-Pros (1:100, mAb MR1A DSHB; Campbell *et al.* 1994), mouse anti-Boss (1:1000, gift from S. L. Zipursky; Cagan *et al.* 1992), mouse anti-Cyclin A (1:10, A12 from DSHB, a gift of I. Hariharan; Knoblich and Lehner 1993), mouse anti-Cyclin B (1:50 F2F4 from DSHB, gift of I. Hariharan; Knoblich and Lehner 1993), mouse anti-Cyclin D [1:10, gift of K. Moberg (unpublished data)], rabbit anti-phospho histone H3 (1:1000, Cell Signaling Technologies 9701), rat anti-Ci155 (1:1, 2A1, gift of R. Holmgren; see Motzny and Holmgren 1995), rabbit anti-Hedgehog (1:625, gift of I. Guererro), rabbit anti-pMad (1:500, gift of T. Tabata; Persson *et al.* 1998), mouse anti-Notch intracellular domain (1:200, from DSHB, gift of K. Moberg), guinea pig anti-Eyg (1:200, gift of K. Moberg) and rabbit anti-Lamin (1:1000, gift of D. Kiehardt). The secondary antibodies were from Jackson ImmunoResearch (West Grove, PA) and were goat anti-mouse Cy5 (1:500, 115-175-003), goat anti-rabbit TRITC (1:250, 111-025-003), goat anti-rabbit HRP (1:100, 111-035-003), goat anti-mouse HRP (1:40, 115-035-003), and goat anti-rat TRITC (1:200, 112-025-003).

Mosaic clones and flow cytometry: mnm^{P} and mnm^{PX1} clones were generated using *ey:FLP* (Newsome *et al.* 2000) or *hs:FLP* (Xu and Rubin 1993). For heat-shock experiments, clones were induced 24, 48, 72, or 96 hr before dissection, by one incubation at 37° for 1 hr. Discs were dissected from wandering third instar larvae. Wing discs were obtained 24 hr after heat shock and flow cytometry was performed as previously described (Tapon *et al.* 2001). The following genotypes were derived for mosaics and/or flow cytometry:

1. $w^{1118}/y^{1}\ w^{1118}$ *ey:FLP*; $P(ry^{+}=neoFRT)42D\ P(w^{+},ry^{+})47A/P(ry^{+}=neoFRT)42D$
2. $w^{1118}/y^{1}\ w^{1118}$ *ey:FLP*; $P(ry^{+}=neoFRT)42D\ P(w^{+},ry^{+})47A/P(ry^{+}=neoFRT)42D\ mnm^{P}$
3. $w^{1118}/y^{1}\ w^{1118}$ *ey:FLP*; $P(ry^{+}=neoFRT)42D\ P(w^{+},ry^{+})47A/P(ry^{+}=neoFRT)42D\ mnm^{PX1}$
4. w^{1118}/w^{1118} *hs:FLP*; $P(ry^{+}=neoFRT)42D$ P(w^{+mC}=*Ubi:GFP.nls*)2R1 P(*Ubi:GFP.nls*)2R2/$P(ry^{+}=neoFRT)42D$
5. w^{1118}/w^{1118} *hs:FLP*; $P(ry^{+}=neoFRT)42D$ P(w^{+mC}=*Ubi:GFP.nls*)2R1 P(*Ubi:GFP.nls*)2R2/$P(ry^{+}=neoFRT)42D\ mnm^{PX1}$
6. $w^{1118}/y^{1}\ w^{1118}$ *ey:FLP*; $P(ry^{+}=neoFRT)42D$ P(w^{+mC}=*Ubi:GFP.nls*)2R1 P(*Ubi:GFP.nls*)2R2/$P(ry^{+}=neoFRT)42D$
7. $w^{1118}/y^{1}\ w^{1118}$ *ey:FLP*; $P(ry^{+}=neoFRT)42D$ P(w^{+mC}=*Ubi:GFP.nls*)2R1 P(*Ubi:GFP.nls*)2R2/$P(ry^{+}=neoFRT)42D\ mnm^{PX1}$
8. $w^{1118}/y^{1}\ w^{1118}$ *ey:FLP*; $P(ry^{+}=neoFRT)42D$ P(w^{+mC}=*Ubi:GFP.nls*)2R1 P(*Ubi:GFP.nls*)2R2/$P(ry^{+}=neoFRT)42D\ mnm^{PX1}$; P($w^{+mC}$=*mnm transgene*)
9. w^{1118} *GMR:P35*/$y^{1}\ w^{1118}$ *ey:FLP*; $P(ry^{+}=neoFRT)42D$ P(w^{+mC}=*Ubi:GFP.nls*)2R1 P(*Ubi:GFP.nls*)2R2/$P(ry^{+}=neoFRT)42D\ mnm^{PX1}$
10. w^{1118}/w^{1118} *hs:FLP*; $P(ry^{+}=neoFRT)42D$ P(w^{+mC}=*Ubi:GFP.nls*)2R1 P(*Ubi:GFP.nls*)2R2/*FRT42D* mnm^{PX1};*hh:GAL4*/UAS:*P35*.

NCBI accession numbers:

Drosophila melanogaster (Mnm): AAD34765.1
Homo sapiens (RBBP6): NP_008841.2
Mus musculus (PACT/P2P-R): AAC72432.1
Caenorhabditis elegans: T21861
Arabidopsis thaliana: NP_199554.1
Schizosaccharomyces pombe: NP_596522.1
Saccharomyces cerevisiae (Mpe1): NP_012864.1

RESULTS

***mini-me* is a dominant genetic enhancer of *hedgehog* in the developing eye:** We undertook a genetic screen to discover genes that interact with *hedgehog* (*hh*) in the developing Drosophila eye, using a viable heteroallelic genotype. hh^{8} (also known as hh^{13C}) is a homozygous lethal allele (Mohler 1988; Porter *et al.* 1995) and hh^{8} heterozygous eyes are phenotypically indistinguishable from wild type (Figure 1A). hh^{bar3} is a homozygous viable allele (Ives 1950; Mohler 1988) and has a strong recessive eye phenotype with an indented anterior side (arrow in Figure 1B and Lee *et al.* 1992). The hh^{8}/hh^{bar3} heterozygote has an intermediate eye phenotype, with no anterior indentation (arrowhead in Figure 1C). We used the hh^{8}/hh^{bar3} heterozygote as the basis for the genetic screen.

We treated isogenized hh^{bar3} homozygous males with the chemical mutagen EMS and crossed them to isogenized hh^{8} balanced females. We screened ~10,000 F_1 males for modified eye phenotypes and recovered 62 mutations in 49 autosomal loci (by noncomplementation for lethality). Mutations were recovered in nine known genes with effects on embryonic development: *Egfr*, *even skipped*, *gooseberry*, *huckebein*, *odd paired*, *patched*, *smoothened*, *thickveins*, and *tramtrack* (Nüsslein-Volhard and Wieschaus 1980). These included members of the *hedgehog* pathway, the receptor component genes *patched* and *smoothened*, (Lum and Beachy 2004) as well as genes known to act in pathways also associated with eye development, the *decapentaplegic* and *Egfr* pathways (Heberlein and Moses 1995; Freeman 1997; Voas and Rebay 2004). In addition, we recovered mutations

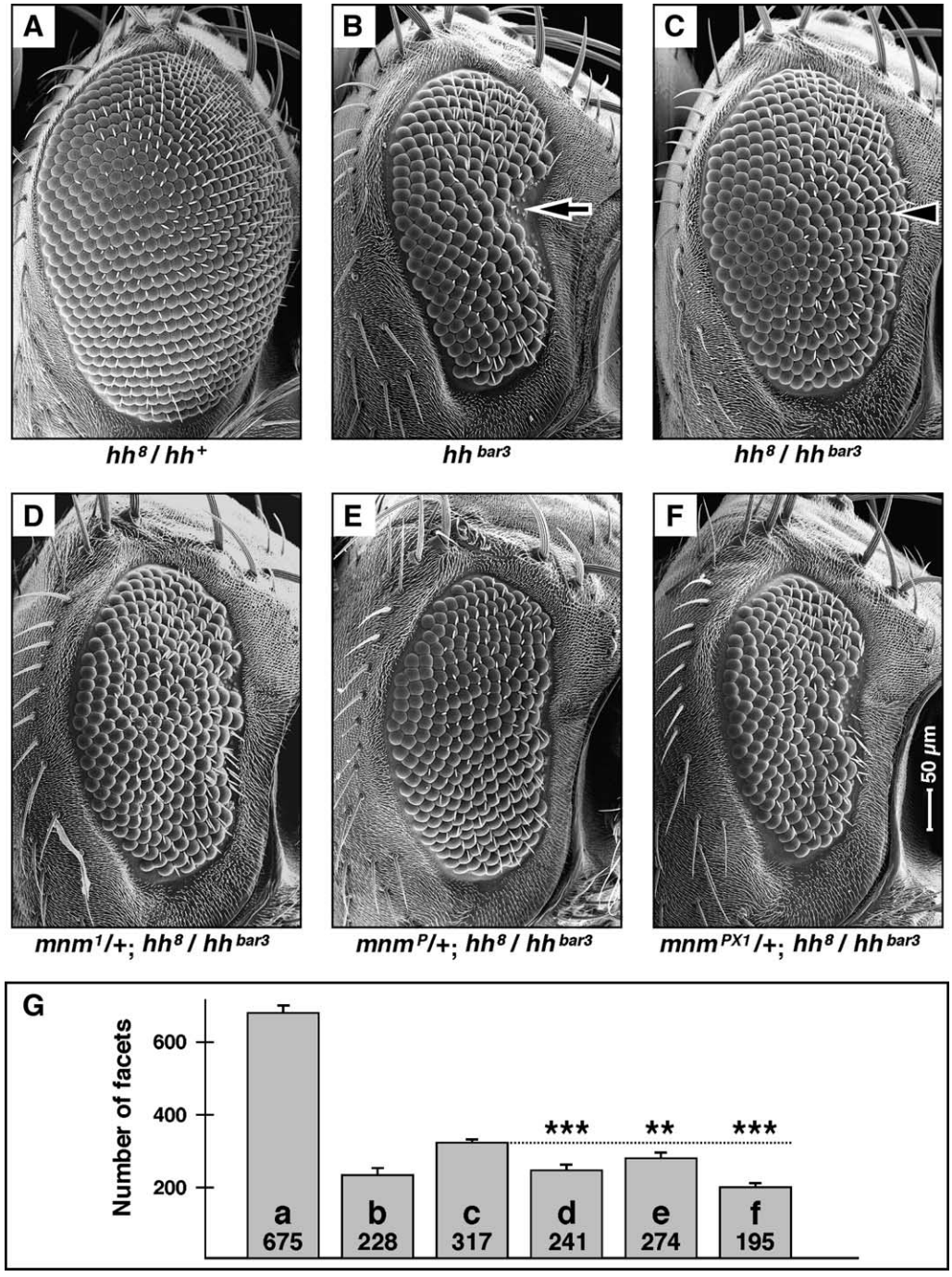

FIGURE 1.—*mnm* loss-of-function is a dominant enhancer of *hedgehog* loss-of-function in the compound eye. (A–F) Scanning electron micrographs of adult female compound eyes: dorsal, up; anterior, right and to the same scale (indicated in F). (A) hh^{8}/hh^{+}, phenotypically indistinguishable from wild type; (B) hh^{bar3}/hh^{bar3}, has a rough and reduced eye; (C) hh^{8}/hh^{bar3}, has a slightly rough and reduced eye; (D) $mnm^{1}/+$; hh^{8}/hh^{bar3}; (E) $mnm^{P}/+$; hh^{8}/hh^{bar3}; (F) $mnm^{PX1}/+$; hh^{8}/hh^{bar3}. Note that the *hedgehog* eye phenotype is enhanced by *mnm* loss-of-function. (G) Quantification of facet counts; also see MATERIALS AND METHODS. The number in each bar is the mean number of facets and the letter identifies which genotype and section (as above) it refers to. Error bars are standard deviation. $***P < 0.005$; $**P < 0.01$.

in 40 loci that we could not identify by complementation testing to known mutations. This article is focused on one of these: *En(hh)2A*. For reasons explained below, we named this EMS-induced allele *mini-me*^{1} (*mnm*^{1}, Figure 1D).

Molecular characterization of *mnm*: *mnm*^{1} fails to complement the lethality of *l(2)rQ313*^{rQ313}, which is a P(PZ) insertion recovered in a screen for P-induced lethals (SPRADLING *et al.* 1999). The *P*-element lies in the first intron of a cytogene (*CG3231*, Figure 2A), immediately to the left of *genghis khan* (*gek*) (LUO *et al.* 1997). We renamed *l(2)rQ313*^{rQ313} *mnm*^{P}. We obtained an embryonic 3937-bp cDNA from Research Genetics (LD21643). There are nine exons containing an open reading frame that encodes a 1231-residue protein (Figure 2, A and B).

We found that *mnm*^{1} is a late pupal lethal, while *mnm*^{P} dies in stage 16 of embryogenesis. We suspected that one or both alleles might not be a null and there was no large deletion available for the region, so we excised the *P* element to generate *mnm*^{PX1}, which removes the start of the open reading frame and three of the most conserved protein domains (Figure 2A). *mnm*^{PX1} is an embryonic lethal and we take it to be a null. *mnm*^{P} and *mnm*^{PX1} are also dominant enhancers of the hh^{8}/hh^{bar3} eye

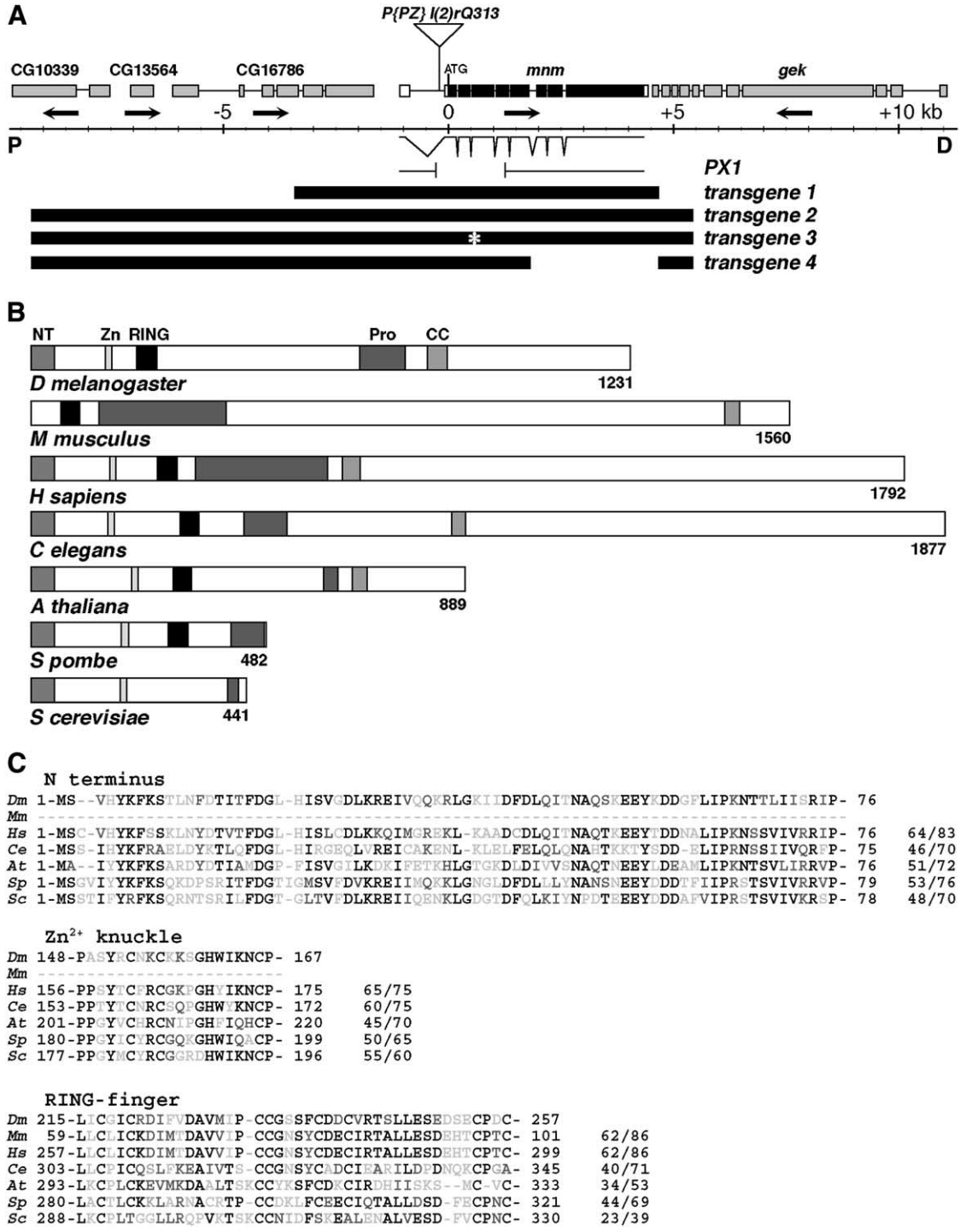

FIGURE 2.—Molecular-genetic characterization of the *mnm* locus. (A) Map of the *mnm* region, in polytene region $60B_{8–11}$: proximal ("P") is left; distal ("D") is right; center is a genomic scale, marked in kilobases. Orientations of transcription units are indicated by arrows: *CG10339, CG13564* and *CG16786* (deduced from genomic sequence), *mnm* (*CG3231*), and *genghis khan (gek).* The position of the insertion of P(PZ) *l(2)rQ313* is indicated. Exon/intron structure of the *mnm* cDNA (clone LD21643) is shown. The structure of the 1488-bp deletion in mnm^{PX1} is indicated. Below this are the structures of four transgenes, as described in the text. (B) A comparison between the deduced Drosophila Mini-me protein domain structure and the closest homologs in other species: *M. musculus* (mP2P-R), *H. sapiens* (hRBBP6), *C. elegans*, *A. thaliana*, *S. pombe*, and *S. cerevisiae* (Mpe1). Conserved domains: NT, N-terminal domain; Zn, Zinc knuckle; RING, RING finger, Pro, proline rich; and CC, coiled coil. (C) Amino acid sequence alignments of three of the conserved domains, as indicated. Species are as in B. Residue numbers are indicated, and the percentages of identity/similarity to Mnm are given. Solid residues are identical, residues with dark shading are conservative changes, and residues with light shading are unconserved changes.

phenotype (Figure 1, E and F) and this enhancement is statistically significant (Figure 1G).

The phenotypic effects of all three *mnm* lesions (the EMS, P, and excision deletion) could be through a *cis* effect on one of the flanking genes. We were able to exclude *gek* by complementation, but could not likewise eliminate *CG16786*, the gene to the left (as no mutations are known for it). We attempted to rescue *mnm* function using an 8-kb genomic fragment (transgene 1, Figure 2A), as this includes both ends of the cDNA, but it does not rescue *mnm* lethality. A longer 14.7-kb genomic fragment (transgene 2, Figure 2A) does rescue the lethality associated with the mnm^{P} and mnm^{PX1} chromosomes, but not mnm^{1}. It may be that the mnm^{1} chromosome contains a second lethal lesion, but we could not rescue any heteroallelic combination containing mnm^{1}. RT–PCR analyses of *mnm* embryos suggest that mnm^{1} may be a hypermorphic or neomorphic allele (Figure 3B, see below). Transgene 2 also rescued the eye development defects of mnm^{P} and mnm^{PX1} (see below). On the basis of the argument that mnm^{PX1} is a single-gene null, we suggest that transgene 2 contains all the genomic sequences required for *mnm* genetic function.

However, transgene 2 includes the entire predicted coding sequences of both *CG3231* and *CG16786* and thus does not eliminate either gene as a candidate for *mnm*. So we tested two derivatives of transgene 2 that selectively knocked out *CG3231* function: transgene 3 includes an engineered 4-base mutation (a predicted frameshift in *CG3231*, Figure 2A), and transgene 4 includes a deletion that terminates *CG3231* after amino acid 491 (Figure 2A). While transgene 2 rescues the lethality of the *mnm* null mutation, transgenes 3 and 4 do not. Thus, *CG3231* is required for *mnm* function and we henceforth refer to *CG3231* as *mnm* (Figure 2A).

The deduced Mnm protein contains several conserved domains (Figure 2, B and C). The first 76 amino acids form a previously uncharacterized but conserved N-terminal domain (NT). The closest human homolog, retinoblastoma binding protein 6 (RBBP6), contains the NT domain (Figure 2C and Sakai *et al.* 1995). The closest murine homolog is PACT/P2P-R (Simons *et al.* 1997; Witte and Scott 1997) and reported partial cDNAs do not encode the NT domain, but this domain is encoded in the genomic sequence (although we have not shown it in Figure 2, B and C). Following the NT domain is a conserved "zinc-knuckle" domain, thought to be involved in nucleic acid binding (Summers 1991). A "RING finger" domain often associated with Ubiquitin ligases is conserved in the human and mouse homologs (Figure 2, B and C; Freemont 2000). There are also protein-interaction motifs: proline-rich (Pro) and coiled-coil (CC) domains (Mason and Arndt 2004).

S. cerevisiae has a genetically characterized homolog of *mnm* called *Mpe1* (Vo *et al.* 2001), shown to function in polyadenylation. Uncharacterized *mnm* homologs are present in the published genome sequences of *C. elegans*, *A. thaliana*, and *S. pombe*. All of the homologs, except ScMpe1, share all the conserved domains (Figure 2B).

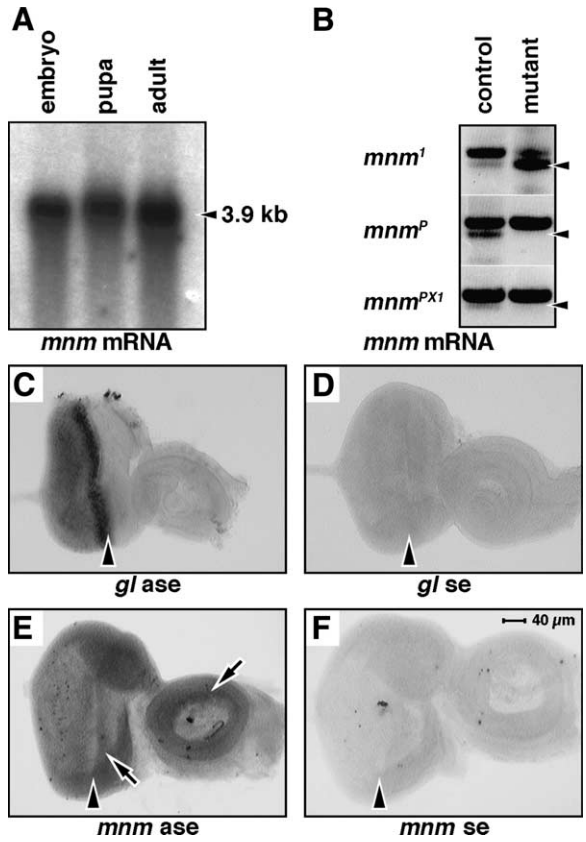

Figure 3.—*mnm* expression. (A) RNA gel blot, stages as indicated. *mnm* mRNA is indicated by an arrowhead. (B) RT gel. RNA from single embryos was isolated and analyzed by RT–PCR using gene-specific *mnm* primers. The arrowheads mark the predicted RT product in all sections. The top band in all sections is the predicted product from genomic DNA remaining in the reaction. Genotypes are mnm^{1}/CyO and mnm^{1} (top), mnm^{P}/CyO and mnm^{P} (middle), and mnm^{PX1}/CyO and mnm^{PX1} (bottom). There was no detectable transcript in mnm^{P} or mnm^{PX1} homozygote embryos compared to the heterozygote controls (middle and bottom sections). The *mnm* transcript appeared to be overexpressed in the mnm^{1} homozygote embryos compared to controls (top), suggesting that mnm^{1} may be a hypermorphic or neomorphic allele. (C–F) RNA *in situ* hybridization experiments: (C) *glass* antisense, (D) *glass* sense, (E) *mnm* antisense, and (F) *mnm* sense. Third instar eye-imaginal discs: anterior right, to the same scale indicated in F. The morphogenetic furrow is indicated by an arrowhead. Note the elevated expression of *mnm* mRNA in the eye field and in parts of the antenna (arrows in E).

Expression of *mnm*: To characterize the temporal expression of *mnm*, we prepared poly(A)$^{+}$ RNA from embryos, larvae, and adults and probed a gel blot, using the *mnm* cDNA as the probe. There is a single major transcript at ~3.9 kb that persists throughout development, confirming the predicted size of the transcript (Figure 3A). In very long exposures, we can also detect an uncharacterized 1.8-kb minor transcript (not shown).

RNA was isolated from single *mnm* heterozygote or homozygote mutant embryos (genotyped using a GFP

balancer chromosome) and used as templates for RT–PCR. RT–PCR products were resolved by agarose gel electrophoresis (Figure 3B). While *mnm*-specific primers were able to detect the predicted product in an mnm^{P} heterozygote embryo (Figure 3B, arrowhead, middle, left lane), no transcript was detected in mnm^{P} homozygote embryos (Figure 3B, middle, right lane). There was also no detectable *mnm* transcript in mnm^{PX1} homozygote embryos compared to the heterozygote control (Figure 3B; bottom, left and right lanes). The *mnm* transcript appeared to be overexpressed in the mnm^{1} homozygote embryos compared to controls, suggesting that mnm^{1} may be a hypermorphic or neomorphic allele (Figure 3B; top, left and right lanes).

As a positive control, we used RNA *in situ* hybridization to visualize the expression of a known gene in the developing eye (*glass*, Figure 3C; Moses *et al.* 1989). We find that *mnm* mRNA is expressed across the entire eye field as well as a ring in the antennal disc (arrows, Figure 3E); this is clearly above the background level (sense strand control, Figure 3F). The level of *mnm* mRNA appears slightly elevated anterior to the furrow.

We attempted to generate specific antibodies to the Mnm protein by two approaches. Neither rabbit polyclonal antisera raised against two Mnm peptides nor antisera against Mnm–GST fusion proteins showed any specificity for the Mnm protein by mosaic clonal analyses (not shown). We conclude that the mRNA *in situ* hybridization experiments reveal the true expression pattern of *mnm* mRNA, because we have controlled for nonspecific expression through the sense strand control.

***mnm* mRNA expression is regulated by *hedgehog* signaling:** While we originally identified *mnm* as a dominant enhancer of *hedgehog*, the genetic and regulatory relationships between the two genes are not at all clear. As *hedgehog* functions to induce many events in the furrow and influences the activities of several other signaling pathways (including Decapentaplegic, Notch, and Egfr) any regulatory relationship may be indirect.

To characterize the relationship between *mnm* and *hedgehog*, we used a conditional, temperature-sensitive allele of *hedgehog*, hh^{ts2} (Ma *et al.* 1993) to remove *hedgehog* function. In $hh^{ts2}/+$ (phenotypically wild-type) discs, no signal was detected with a *mnm* sense strand control (Figure 4A) and normal signal was seen in $hh^{ts2}/+$ discs with the *mnm* antisense probe (Figure 4B). However, in hh^{ts2}/hh^{ts2} homozygous siblings taken from the same vial after 4 hr at 29° (the nonpermissive temperature) the *mnm* signal was absent (Figure 4C). Thus the level of *mnm* transcript is sensitive to *hedgehog* function. While loss-of-*hedgehog* function clearly does affect *mnm* expression, the effect is global (the entire eye and antennal discs) and not limited to the territories in which Hedgehog signals are known to be received (*e.g.*, anterior to the furrow). This may argue for an indirect mechanism for *hedgehog* regulation of *mnm* through the activation of other pathways (see below).

It was possible that *mnm* acts upstream of Hedgehog protein expression or downstream of Hedgehog activation. To test these possibilities, we induced GFP-negatively marked, mnm^{PX1} null homozygous clones in the developing eye, which have normal levels and localization of Hedgehog protein (arrows in Figure 4, D–F). Similarly, we stained retinal mnm^{PX1} clones for the Hedgehog signaling-activated transcription factor, Cubitus interruptus (Ci) but see no changes (arrows in Figure 4, G and H). Taken together these data strongly suggest that *mnm* is not genetically upstream but rather may be downstream of Hedgehog signaling and is controlled at the transcriptional level.

***mnm* is required for cell proliferation and survival in the developing eye:** We used *ey:FLP* (Newsome *et al.* 2000) to induce *mnm* homozygous mutant clones, marked by $white^{-}$, in the developing eye. These were negatively marked in the adult by $white^{+}$. Wild-type control clones were large and occupied roughly half of the eye (arrow in Figure 5A), as did clones homozygous for mnm^{P} (arrow in Figure 5B). However, clones for the deletion allele mnm^{PX1} were largely absent in the adult retina, leaving only scars (arrow in Figure 5C). In retinal sections, wild-type, mnm^{P}, and mnm^{PX1} clones all contained $white^{-}$ photoreceptor cells (arrows in Figure 5, D–F), although there were very few in mnm^{PX1} clones (Figure 5F). These data suggest that *mnm* null cells either do not proliferate or die in the developing eye. However, the detection of some persistent *mnm* null cells suggests that *mnm* null cells may have differential requirements for survival.

To investigate whether *mnm* null cells can differentiate normally, we derived *ey:FLP*-induced mnm^{PX1} homozygous mutant clones that were negatively marked by GFP. In late larval discs we observed small mnm^{PX1} clones that were positive for the neural-specific protein Elav (arrows in Figure 5, G–I), suggesting that there is a strong effect of the *mnm* null mutation on cell number, but perhaps no effect on differentiation (see below). We also found that transgene 2 (see above) can fully rescue this cell number defect (arrows in Figure 5, J–L).

***mnm* null cells are underrepresented and die in proliferative tissue, but have no detectable defects in nonproliferative tissue:** The small size of the *ey:FLP*-induced *mnm* null clones in larval discs could be due to defects in cell proliferation, growth, or survival. To distinguish between these possibilities, we used *hs:FLP* to induce clones and then examined their progeny, in the retina, at a series of times after induction.

mnm null clones induced 24 hr before dissection are frequent, small, and similar in size (about two to four cells) to their adjacent wild-type twin spots (not shown). By 48 hr after induction, *mnm* null clones and wild-type twin spots are seen posterior to the furrow (postmitotic territory, Figure 6A: mutant, black arrows; twin spot, white arrow), but in the region anterior to the furrow, the twin spots grow larger while the mutant clones are

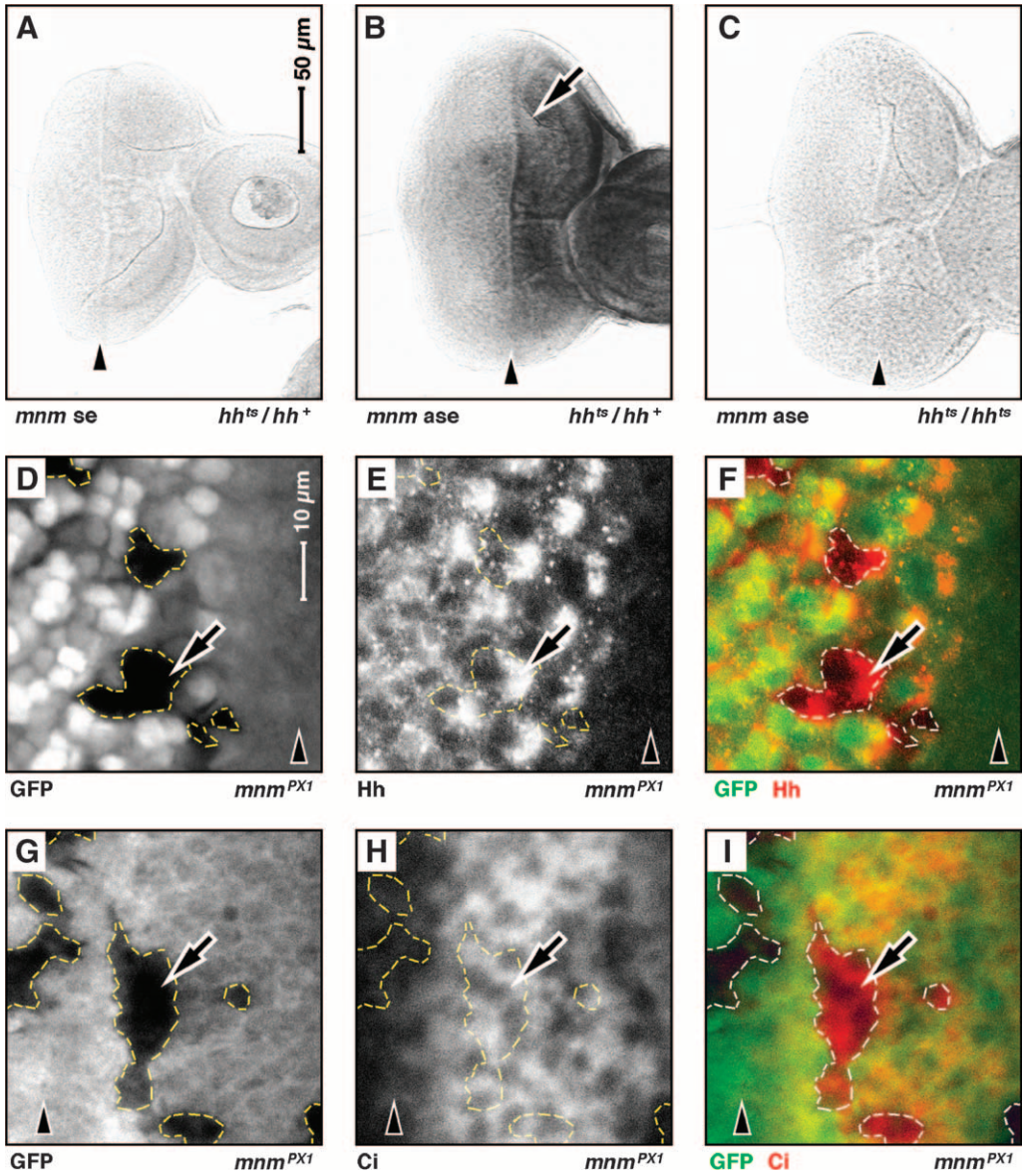

FIGURE 4.—*mnm* is genetically downstream of *hedgehog* signaling. Third instar eye-imaginal discs: anterior, right. A–C and D–I are to the same scale; see bars in A and D. Arrowheads indicate the position of the morphogenetic furrow. (A–C) RNA *in situ* hybridization experiments: (A) $hh^{ts2}/+$, *mnm* sense (se) strand control; (B) hh^{ts2} heterozygote, *mnm* anti-sense (ase) strand [note elevated level of *mnm* mRNA anterior to the morphogenetic furrow (arrow)]; (C) hh^{ts2}/hh^{ts2}, *mnm* anti-sense strand (*mnm* signal is lost in hh^{ts2}/hh^{ts2} animals raised at the nonpermissive temperature). (D–I) Mosaic clones of mnm^{PX1} cells. Clones are negatively marked with GFP and are outlined (white in D and G and green in F and I). E (in white) and F (in red) show the expression of Hedgehog antigen. Note that Hedgehog is not lost from mnm^{PX1} mutant cells (arrow). H (in white) and I (in red) show the expression of activated Ci antigen. Note that activated Ci is not lost from mnm^{PX1} mutant cells (arrow).

lost (a proliferative territory, yellow arrow in Figure 6A). A day later (72 hr after induction) the *mnm* null clones are rare, small, and found only posterior to the furrow (postmitotic territory, black arrow in Figure 6B). The twin spots are large (white arrows in Figure 6B) and often not associated with a null clone. By 96 hr, only large twin spots are seen (white arrow in Figure 6C) and *mnm* null clones are not found. These data suggest that the defects seen in the *hs:FLP* clones take ~48 hr to begin to develop; thus, *mnm clones* can survive one or two cycles of cell division, perhaps through perdurance of the Mnm protein. It should be noted that 72 hr before dissection, all the cells were in a proliferative territory (the furrow had not initiated yet), so the lack of remaining posterior null clones may be due to their deaths between 48 and 72 hr after induction.

If the primary effect of *mnm* loss-of-function is to direct cells to apoptotic death, we might expect to observe a marker of cell death in the clones. We used an activated Caspase3 stain to detect apoptotic cell death and found staining close to, but not always contained within, *mnm* clones that lie anterior to the furrow (proliferative territory, arrows in Figure 6D). Dying cells delaminate from epithelia in the developing wing (GIBSON and PERRIMON 2005; SHEN and DAHMANN 2005), so we suggest that this stain is associated with both dying cells and debris remaining from dead cells that have been extruded. We never see such stain posterior to the furrow (asterisk in Figure 6D), suggesting that *mnm* apoptotic death is limited to the anterior, proliferative domain.

In addition, if the primary effect of *mnm* loss-of-function is to direct cells to apoptotic death, then inhibiting apoptosis might rescue the size of the clones. Thus we induced *mnm* clones in the eye disc in the presence of the baculovirus P35 protein (a potent

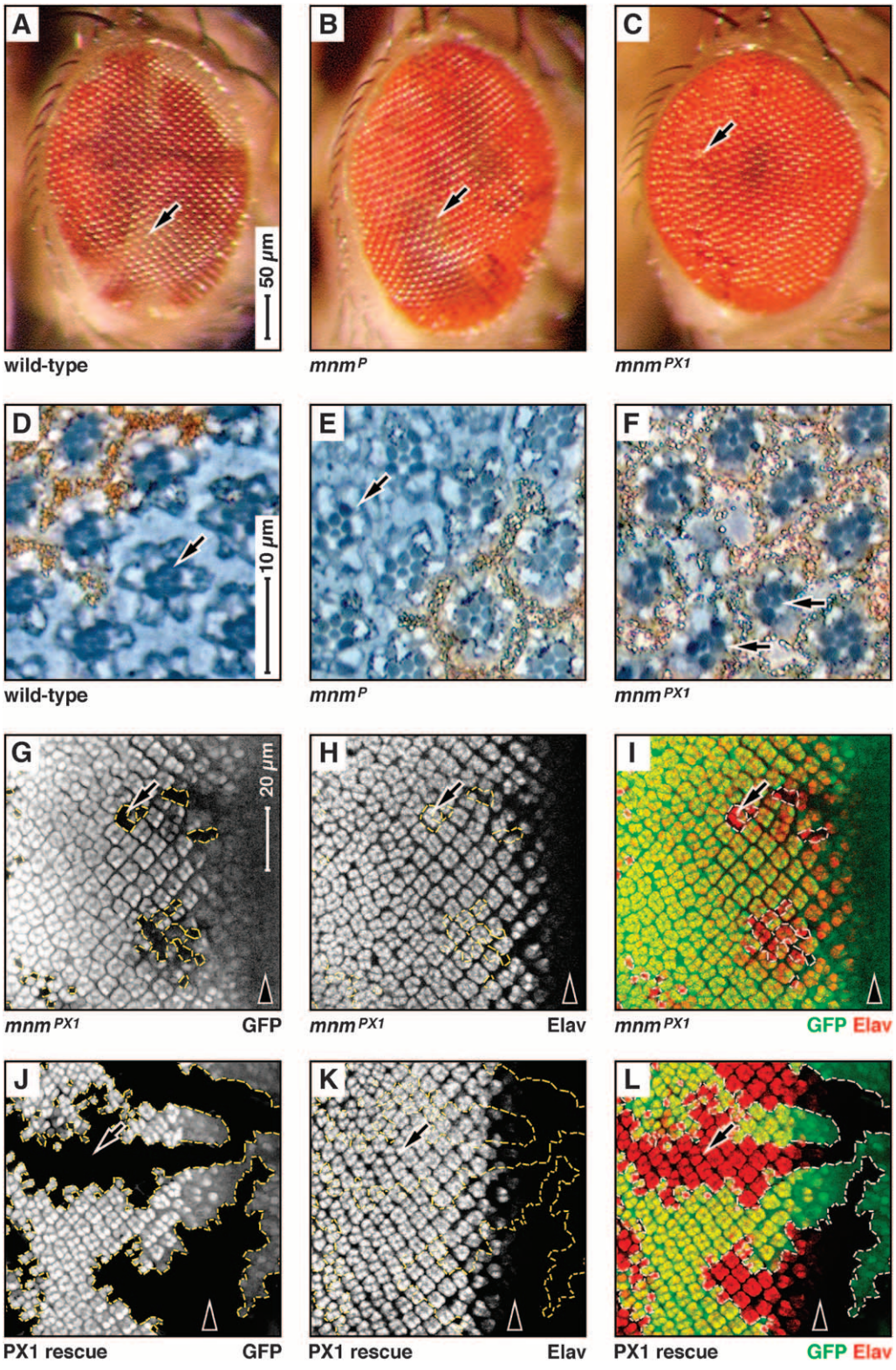

FIGURE 5.—*mnm* loss-of-function affects eye development. (A–C) Scanning electron micrographs of female adult compound eyes containing *ey:Flp*-induced mosaic clones marked by *white*: dorsal, up; anterior, right; scale indicated in A. Genotypes: (A) wild type, (B) mnm^{P}, and (C) mnm^{PX1}. Note that the weak allele mnm^{P} clones are as large as wild type (arrows in A and B) but that the null allele mnm^{PX1} leaves scars (arrow in C). (D–F) Sections of adult compound eyes containing *eyeless:Flp*-induced mosaic clones marked by *white*: dorsal, up; anterior, right; scale indicated in D. Genotypes: (D) wild type, (E) mnm^{P}, and (F) mnm^{PX1}. Note that the wild-type and *mnm* clones contain mutant (*white*$^{-}$) photoreceptor cells (arrows in D–F). (G–L) Third instar eye-imaginal discs containing *eyeless:Flp*-induced mnm^{PX1} mosaic clones (outlined), negatively marked by GFP; anterior, right and to the same scale (bar in G). Arrowheads indicate the position of the morphogenetic furrow. (G and J) GFP in white; (H and K) Elav antigen in white; (I and L) GFP in green and Elav in red. Note that mnm^{PX1} clones are small, but express the differentiation marker Elav (arrow in G–I). (J–L) *mnm* rescuing transgene (see text). Note that the size of the mnm^{PX1} clones is entirely rescued (arrows).

inhibitor of cell death), driven by the GMR enhancer posterior to the furrow in the developing eye, but the size of *mnm* mutant clones was unchanged (data not shown and see HAY *et al.* 1994). These data are consistent with our observations that the apoptotic marker, activated Caspase3, is associated only with *mnm* clones that are anterior to the furrow (Figure 6D). However, this P35 experiment does not test for the effects of cell death anterior to the furrow (because GMR:P35 is expressed only on the posterior side).

Similarly, *mnm* mutant cells in the developing wing disc are small and rarely detectable beyond 48 hr of

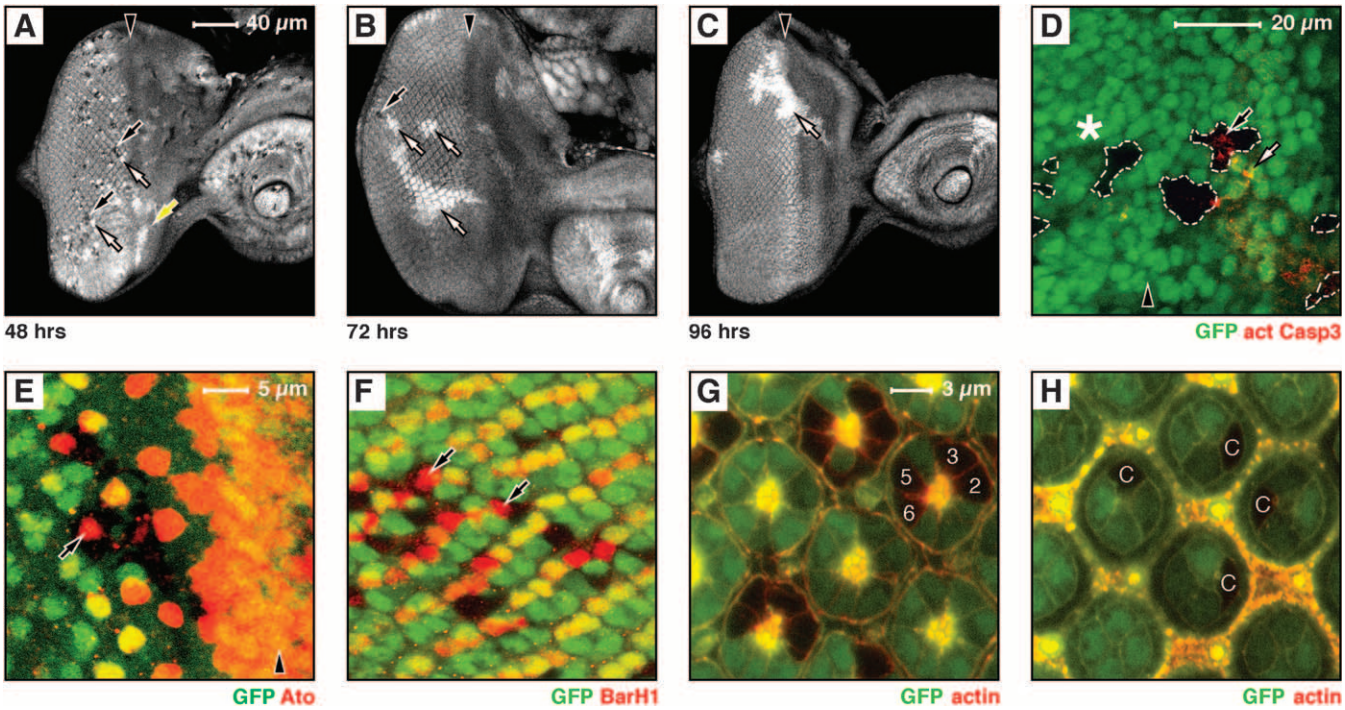

Figure 6.—*mnm* is required for the survival of proliferating cells in the developing eye. (A–H) Eye-imaginal discs containing mnm^{PX1} mosaic clones, negatively marked by GFP; anterior, right. (A–F) Late third instar eye discs; (G–H) 48-hr pupal eye discs. A–C are to the same scale (bar in A), D is at higher magnification (see bar), E and F are to the same scale (bar in E), and G and H are to the same scale (bar in G). Arrowheads indicate the position of the morphogenetic furrow in A–E. (A–C) *hs:FLP*-induced clones, with the induction time before dissection indicated below: (A) 48 hr, (B) 72 hr, and (C) 96 hr. (A–C) GFP is shown as white. Note that 48 hr after induction (A) many small mnm^{PX1} homozygous clones are seen (black clones and black arrows) together with their homozygous wild-type twin spots (white twin spots and white arrow) posterior to the furrow. Note that the twin spots immediately anterior to the furrow lack clones (white twin spots and yellow arrow). At 72 hr (B) only very rare and small mutant clones are seen (black arrow) and the twin spots are far larger than the clones (white arrows). By 96 hr (C) only twin spots are seen (white arrow). (D) Activated Caspase3 antigen within (black arrow) or near (white arrow) mnm^{PX1} clones, anterior to the furrow. Note that there is no activated Caspase3 staining associated with *mnm* clones posterior to the furrow (asterisk). (E) Atonal antigen (red) and (F) BarH1 antigen (red) expressed within mnm^{PX1} clones (arrows). G and H show that mnm^{PX1} mutant cells can persist into pupal life and can differentiate normally [numbers indicate examples of R cell types (G) and cone cells (H)].

clone induction, as in the eye (not shown). We never observe activated Caspase3 in these wing clones, nor is their size rescued by the local expression of P35 (expressed in the posterior compartment using *hh:Gal4*, data not shown). In this wing experiment, we express P35 in the same territory in which the clones develop their size defect. Thus we suggest that the primary defect that produces the small clone size is not apoptotic cell death.

If *mnm* clones are small due to competition effects, then conferring a growth advantage on *mnm* mutant clones might overcome the small clone phenotype. We derived eye imaginal discs with *mnm* clones surrounded by *Minute* heterozygous cells. However, we did not recover any *mnm* mutant tissue surviving beyond 48 hr (not shown).

If *mnm* were to affect cell growth, then we might expect to find that *mnm* cells grow more slowly than wild-type cells. Because we could not inhibit cell death in *mnm* cells by overexpressing P35 (*GMR::P35* or *hh::P35*, see above), we could not accurately determine the growth rate of *mnm* cells. We examined the sizes of persisting *mnm* null cells to determine if *mnm* loss-of-function had any effect on cell size. *mnm* null cells do not appear any smaller than their neighbors (Figure 6, G and H). Furthermore, we counted cells in mutant clones (by marking their nuclei through anti-Lamin D staining) and find that the number of cells per unit area is also not affected (not shown). It is possible that *mnm* cells can compensate for a slower growth rate by slowing their cell cycle time, and thus we are not able to use cell size as a measure of cell growth. However, we cannot conclude that *mnm* has any role in regulating cell growth.

Taken together these data suggest that it is unlikely that the *mnm* clones posterior to the furrow are small due to local apoptosis or competitive effects. Rather, we propose that *mnm* is required for cell survival in the proliferating cells anterior to the furrow in the eye and more generally in the wing (see below).

Surviving *mnm* null cells posterior to the furrow can differentiate and persist into later life: We stained for

several cell-type markers in surviving induced *mnm* homozygous clones and these appear normal (Atonal for R8 photoreceptors in Figure 6E; BarH1 for R1 and R6 in Figure 6F; and Boss, Sevenless, Prospero, and Cut, data not shown). Moreover, *mnm* null cells are found as morphologically normal photoreceptors (Figure 6G) and accessory cells (Figure 6H) 48 hr after puparium formation. These data are consistent with our observations that *mnm* cells are present in the adult eye and stain positively for neural-specific Elav in *ey:FLP*-induced clones in the eye disc (Figure 5, G–I). Thus, we conclude that *mnm* does not control cell-type specification or differentiation.

***mnm* affects nucleic acid content:** Our data are consistent with a function for *mnm* in proliferative cells in the eye and wing, with a secondary effect on survival. To examine the cell cycle profiles of *mnm* mutant cells, we used the developing wing disc as a rich source of proliferating cells. The use of wing rather than eye disc cells for FACS analysis also has the benefit of avoiding artifacts associated with the specific morphologies of the differentiating retinal cells posterior to the morphogenetic furrow. We used *hs:FLP* to induce negatively GFP-marked *mnm* null clones in the wing disc and 24 hr later (at least 24 hr before we observe small *mnm* clones in the wing disc), we dissected and dissociated wing imaginal discs for FACS, as described by Tapon *et al.* (2001). In control discs (in which both the GFP$^+$ and GFP$^-$ cells are *mnm*$^+$), we detect well-superimposed nucleic acid content profiles, which represent the G1, S, and G2/M phases of the cell cycle (Figure 7A). However, *mnm* null cells (blue curve, Figure 7B) are strongly shifted to the right, toward higher nucleic acid content compared to GFP$^+$ *mnm*$^+$ cells in the same discs. Moreover, *mnm* cells appear to accumulate DNA beyond 4N (blue curve, Figure 7B). Forward scatter profiles of *mnm* mutant cells are similar to those of wild-type cells (not shown), consistent with our observation that cell size is not affected in *mnm* mutant cells.

We stained *mnm* null clones in the developing eye for cell cycle markers to test for a specific stage defect: Cyclin E for G1 (Figure 7C, as well as Cyclin D, data not shown), BrdU incorporation for S (Figure 7D), Cyclin A for G2 (Figure 7E, as well as Cyclin B, data not shown), and phosphorylated Histone H3 (pH3) for mitosis (Figure 7F). In all cases, we could find some cells expressing these markers in the clones and in roughly the normal frequencies.

***mnm* is a dominant suppressor of *dpp* loss-of-function and *Notch* gain-of-function in the eye:** We examined whether *mnm* loss-of-function could genetically interact with mutations in other signaling pathways that caused adult eye phenotypes, by removing one copy of *mnm* using either the *mnm*^{P} or *mnm*^{PX1} allele. While we observed no effect by either allele on the eye phenotypes of *wg*^{gla}/+, *ellipse*^{B1}/+, *rough*^{D}/+, or *rolled*^{SEM}/+ flies (not shown), we did observe strong suppressive

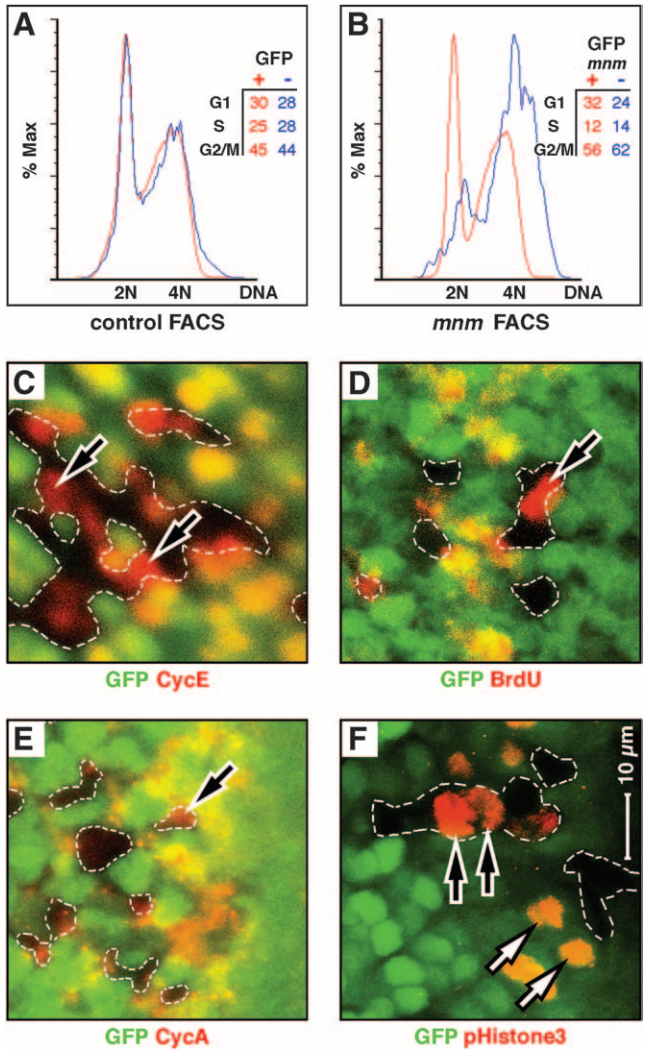

Figure 7.—*mnm* loss-of-function affects cell cycle progression. (A and B) Fluorescence-activated cell sorting (FACS) traces. Red curves are GFP$^+$-expressing cells and blue are GFP$^-$ cells. DNA content (*x*-axes) is plotted against the percentage of maximal absorbance (*y*-axes). Insets show the percentages of cells in each genotype distributed between the phases G1, S, and G2/M. Cells were prepared from third larval wing imaginal discs containing *hs:FLP*-induced, GFP-marked mosaic clones, 24 hr after clone induction. (A) Control discs in which both the GFP$^+$ and GFP$^-$ cell populations are *mnm*$^+$. Note that the red and blue curves are superimposed with major peaks interpreted as 2N and 4N DNA content. (B) Cells prepared from imaginal discs in which the GFP$^+$ cells are either *mnm*$^+$ homozygotes or *mnm*$^+$/*mnm*^{PX1}. As *mnm* is recessive, all the GFP$^+$ cells are phenotypically wild type. The GFP$^-$ cells are *mnm*^{PX1} homozygotes. Note the rightward shift of the GFP$^-$ *mnm* mutant cells, suggesting elevated DNA content, and an increased percentage of cells are scored as G2/M. (C–F) Third instar eye-imaginal discs, with fields shown posterior to the morphogenetic furrow, containing GFP-marked *mnm*^{PX1} homozygous clones. Anterior is to the right and C–F are to the same scale (bar in F). GFP is green and the antigens are in red: (C) Cyclin E (G1 phase), (D) BrdU (S phase), (E) Cyclin A (G2 phase), and (F) phosphorylated Histone H3 (pH3, M phase). Note that *mnm*^{PX1} mutant cells can express all four of these markers (black arrows), indicating that no cell cycle phase is absent.

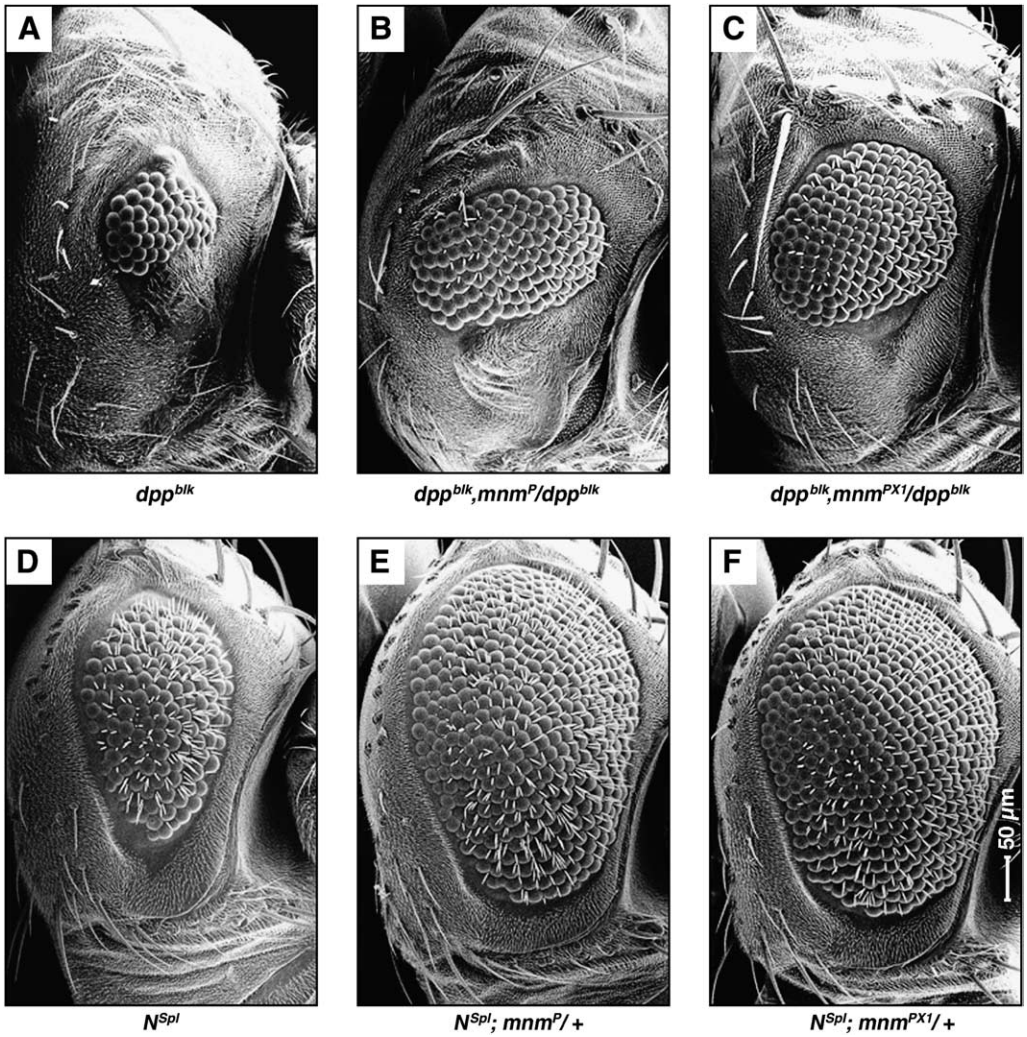

FIGURE 8.—*mnm* dominantly suppresses *dpp* loss-of-function and *notch* gain-of-function in the eye. (A–F) Scanning electron micrographs of adult compound eyes: dorsal, up; anterior, right and to the same scale (indicated in F). (A) dpp^{blk}, small, rough eye with very few facets; (B) dpp^{blk}, mnm^{P}/dpp^{blk}, loss of one copy of mnm^{P} can suppress the small eye size and the eye contains more facets; (C) dpp^{blk}, mnm^{PX1}/dpp^{blk}, the mnm^{PX1} null allele strongly suppresses the small eye phenotype; (D) $Notch^{Spl}$ (N^{Spl}), reduced, rough eye with missing or double bristles; (E) N^{Spl}; $mnm^{P}/+$ and (F) N^{Spl}; $mnm^{PX1}/+$, both the mnm^{P} and the mnm^{PX1} strongly suppress the small-eye phenotype, the null allele to a greater degree.

effects on a loss-of-function mutation in *dpp*, dpp^{blk} (Figure 8, A–C;TREISMAN and RUBIN 1995), and a gain-of-function mutation in *Notch*, $Notch^{Spl}$ (N^{Spl}, Figure 8, D–F; NAGEL and PREISS 1999), by both alleles. To determine whether Dpp or Notch signaling is affected in cells lacking *mnm*, we stained *mnm* null clones in the eye for pMad (target of Dpp signaling; WIERSDORFF *et al.* 1996), the Notch intracellular domain, or eye gone (target of Notch signaling; CHAO *et al.* 2004; DOMINGUEZ *et al.* 2004). However, we saw no effect in *mnm* null clones posterior or anterior to the furrow (not shown). This result was not surprising since we observe no effects on patterning in *mnm* null clones posterior to the furrow; and activated cell death in *mnm* null clones ahead of the furrow leads to cell loss. Altogether, our data suggest that *mnm* may be interacting with some component of these pathways in opposite ways, to antagonize Dpp signaling and enhance Notch signaling functions. Both the Dpp and the Notch pathways interact with Hh signaling during eye development (CURTISS and MLODZIK 2000; FU and BAKER 2003) and might explain the indirect regulation of *mnm* by *hedgehog*.

Excess *mnm* causes overproliferation and melanotic mass formation: We derived transgenic flies that expressed the *mnm* cDNA under the control of the UAS-activating element. *mnm* overexpression was driven by *en:GAL4* in the posterior parasegment compartments; flies were raised at 18°, 25°, or 29° and monitored throughout their lifetime. *mnm* overexpression led to reduced viability in all 10 lines at 18° and larval or pupal lethality at 25° or 29°. Six of the 10 lines exhibited small black melanotic masses in their larval epidermis compared to their sibling controls at 18°, similar to the metastatic masses seen by others (not shown; PAGLIARINI and XU 2003). Adult escapers exhibited gross patterning defects in the engrailed-expressing dorsal abdomen (not shown) and also often contained melanotic masses in the ventral epidermis (arrowhead, Figure 9A). The wings of adult escapers were patterned normally, but were reduced in size in the posterior compartment compared to control (Figure 9, D and G).

One explanation for the small posterior wing phenotype of *en::mnm* flies is increased cell death in the posterior compartment of the developing wing disc. We

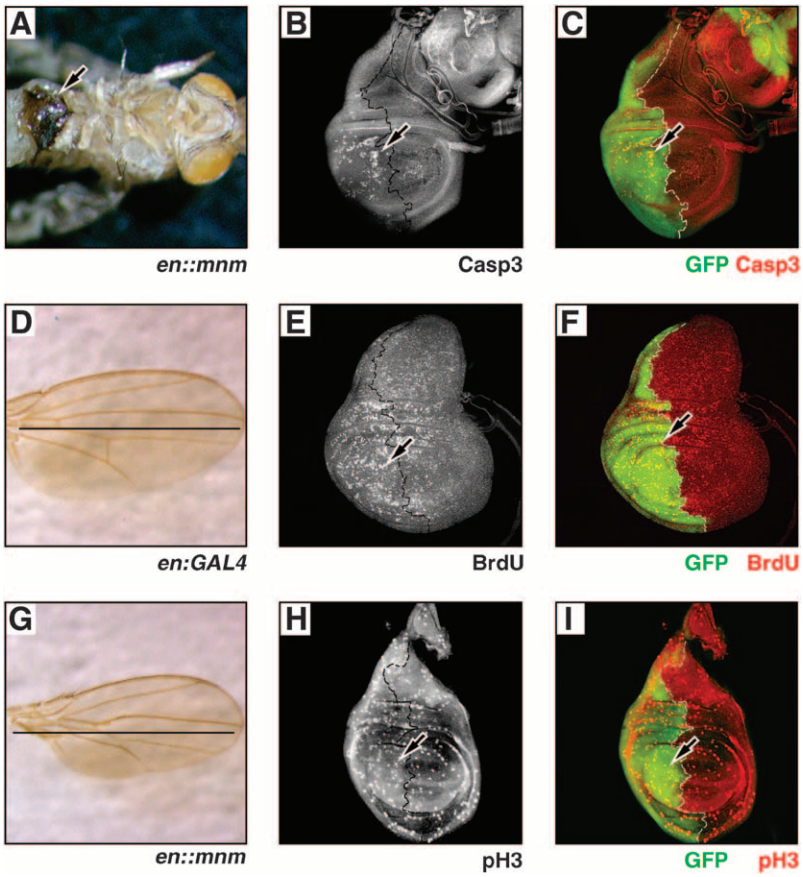

FIGURE 9.—Excess *mnm* causes overproliferation and melanotic mass formation. (A) w^{1118}; *en:Gal4*/UAS:*mnm* pharate adult raised at 18°, ventral side up. Legs have been removed. Arrow marks the melanotic mass in the ventral epidermis. (B, C, E, F, H, and I) *en:Gal4*/UAS:GFP, UAS:*mnm* wing discs obtained from third instar larvae raised at 25°. Arrows mark *mnm*-overexpressing cells in the posterior compartment, black and white dotted lines mark the A–P boundaries; anterior is right. (B and C) Caspase3 (white in B, red in C) and BrdU (white in E, red in F) staining are increased, while phosphorylated Histone H3 (pH3, white in H, red in I) is unaffected in the *en::mnm* posterior compartments. (D) *en:Gal4* control and (E) *en::mnm* adult wings of flies raised at 18°. Black lines mark the A–P boundaries. Note that patterning is unaffected in *en::mnm* wings but the size of the posterior compartment is reduced compared to the control wing.

dissected wing discs from *en::mnm* wandering larvae that were raised at 25° and stained for activated Caspase3. These larvae also contained UAS:GFP to help identify the *mnm* overexpressing domain (Figure 9, C, F, and I). Indeed, there was increased activated Caspase3 staining in the posterior compartment of the *en::mnm* wing discs (Figure 9, B and C).

To determine if *mnm* overexpression could induce proliferation, we also stained *en::mnm* wing discs for BrdU (Figure 9, E and F) and pH3 (Figure 9, H and I). While we observed no appreciable differences in pH3 staining, we did observe more BrdU-positive cells in the posterior compartment in these discs, suggesting that *mnm* overexpression is sufficient to induce cells to proliferate, and this overproliferation likely leads to the activation of programmed cell death.

DISCUSSION

In this study we report the identification of a potential regulator of cell proliferation and survival. The Drosophila *mnm* gene encodes a conserved protein with a novel N terminus and Zinc knuckle, RING finger, and proline-rich and coiled coil domains. *mnm* is expressed everywhere in the developing eye disc and is enriched ahead of the morphogenetic furrow. The expression of *mnm* is dependent upon Hedgehog signaling (perhaps indirectly), as loss of Hedgehog signaling through an inactivating mutation in *hedgehog* greatly reduces its expression.

From our timed analysis of mutant clones, it appears that *mnm* null cells in proliferative regions of the developing eye (and wing) can replicate for two or three times over 48 hr, but between 48 and 72 hr after clone induction they suffer some crisis and die. It may be that this delayed defect is due to perdurance of the Mnm protein. If during that time window they receive developmental signals to cease proliferation and differentiate, they can then survive. The morphogenetic furrow and subsequent events do provide such differentiation signals so that *mnm* null clones can persist in the retina, if they are induced late enough. Our data show that if the furrow passes over *mnm* null cells in the first 24–48 hr after they become homozygous, they can persist to the adult eye, and many differentiate as morphologically normal photoreceptors and accessory cells. Taken together, these data suggest that Mnm is required for some function in proliferative cells, but not in postmitotic cells. Because the *mnm* mutant clones posterior to the furrow can survive and differentiate as apparently perfect, yet tiny copies of their wild-type twin spots, we named the gene "*mini-me*" (MYERS and MCCULLERS 1999).

Our FACS analysis of *mnm* null cells suggests that *mnm* null cells have abnormal nucleic acid content. This could reflect changes in nuclear DNA, mitochondrial

DNA, and/or RNA content. It could be that the *mnm* mutant cells have lost the correct coupling of DNA synthesis to cell division and accumulate DNA beyond 4N. It may be that these cells overreplicate DNA during S phase, missegregate DNA during mitosis, or fail to divide and become aneuploid. *mnm* overexpression is sufficient to induce proliferation; and this excessive proliferation is toxic and leads to cell death. An increase in nucleic acid content associated with *mnm* loss-of-function and the overproliferation of *mnm*-overexpressing cells are consistent with a role for *mnm* as a regulator of mitotic progression, although whether Mnm plays a role in DNA replication, the DNA damage checkpoints, or mitotic entry/exit is not clear.

The closest human and murine homologs of Drosophila Mnm are RBBP6 and PACT/P2P-R. These proteins have been shown to associate with Retinoblastoma (Rb) protein and p53 proteins *in vitro*, which are potent regulators of the cell cycle, including regulating entry into S phase and the monitoring of DNA integrity (Sakai *et al.* 1995; Simons *et al.* 1997). This could be consistent with our suggestion that loss of Mnm may lead to aberrant DNA metabolism. Furthermore P2P-R is downregulated in differentiating cells (Witte and Scott 1997), consistent with our observation of a lack of Mnm function in postmitotic territories in the developing eye. RNAi knockdown of P2P-R in mouse 3T3 cells affects nocodazole-induced arrest and UV-induced apoptosis, also possibly consistent with a disturbance in DNA metabolism (Gao *et al.* 2002; Scott and Gao 2002).

Hedgehog signaling has been implicated in cell cycle regulation in both flies and vertebrates (Forbes *et al.* 1996; Duman-Scheel *et al.* 2002; Roy and Ingham 2002). The link between *hedgehog* and *mnm* may be a new mechanism for this control. However, the interaction between *hedgehog* and *mnm* could be indirect: the small phenotype of *mnm* clones is quite dissimilar to that of *smoothened* clones, which are not small (lacking the Hedgehog receptor; Strutt and Mlodzik 1996). We also observe phenotypic effects of *mnm* loss-of-function outside of the territories where the Hedgehog signal is received. Thus we suggest that while *mnm* may be controlled in part by *hedgehog*, it has much more general functions and is likely, also, to be regulated by other pathways.

It is interesting that loss of *mnm* function strongly interacts genetically with the Dpp and Notch pathways in opposite ways. Both pathways have recently been characterized to have significant roles in regulating cell cycle progression in the developing eye. Dpp signaling promotes G1 arrest, while Notch signaling regulates S-phase entry in the second mitotic wave (Baonza and Freeman 2005; Firth and Baker 2005). It could be that *mnm* is interacting directly with these pathways to regulate cell cycle progression. However, the precise mechanism remains to be resolved.

We thank Philip Beachy for suggesting the *hedgehog* screen genotype; Ken Moberg, Maureen Powers, and the Moses lab for their helpful comments; Summer Cook for technical assistance; B. Edgar, I. Guererro, I. Hariharan, A. Jarman, D. Kiehardt, L. Luo, G. Mardon, K. Moberg, K. Saigu, T. Tabata, R. Holmgren, and S. L. Zipursky for their gifts of reagents; and C. Commisso and G. L. Boulianne for their biochemical help. This work was supported in the Moses lab by a grant from the National Eye Institute (EY09299), R. Reifegerste was supported in part by a Deutsche Forschungsgemeinschaft/German fellowship (RE 1089/1-1), and C. Jones was supported in part by training grants T32GM008367 and T32EY007092 and a supplement to National Eye Institute grant R01EY012537.

LITERATURE CITED

Baker, N. E., 2001 Cell proliferation, survival, and death in the *Drosophila* eye. Semin. Cell. Dev. Biol. **12:** 499–507.

Baker, N. E., and S. Y. Yu, 2001 The EGF receptor defines domains of cell cycle progression and survival to regulate cell number in the developing *Drosophila* eye. Cell **104:** 699–708.

Baonza, A., and M. Freeman, 2005 Control of cell proliferation in the *Drosophila* eye by Notch signaling. Dev. Cell **8:** 529–539.

Blochinger, K., R. Bodmer, L. Y. Jan and Y. N. Jan, 1990 Patterns of expression of Cut, a protein required for external sensory organ development in wild-type and *cut* mutant *Drosophila* embryos. Genes Dev. **4:** 1322–1331.

Brand, A. H., and N. Perrimon, 1993 Targeted gene expression as a means of altering cell fates and generating dominant phenotypes. Development **118:** 401–415.

Cagan, R. L., and D. F. Ready, 1989 The emergence of order in the *Drosophila* pupal retina. Dev. Biol. **136:** 346–362.

Cagan, R. L., H. Krämer, A. C. Hart and S. L. Zipursky, 1992 The Bride of Sevenless and Sevenless interaction: internalization of a transmembrane ligand. Cell **69:** 393–399.

Campbell, G., H. Göring, T. Lin, E. Spana, S. Andersson *et al.*, 1994 RK2, a glial-specific homeodomain protein required for embryonic nerve cord condensation and viability in *Drosophila*. Development **120:** 2957–2966.

Chao, J. L., Y. C. Tsai, S. J. Chiu and Y. H. Sun, 2004 Localized Notch signal acts through *eyg* and *upd* to promote global growth in *Drosophila* eye. Development **131:** 3839–3847.

Curtiss, J., and M. Mlodzik, 2000 Morphogenetic furrow initiation and progression during eye development in *Drosophila*: the roles of *decapentaplegic*, *hedgehog* and *eyes absent*. Development **127:** 1325–1336.

de Nooij, J. C., and I. K. Hariharan, 1995 Uncoupling cell fate determination from patterned cell division in the *Drosophila* eye. Science **270:** 983–985.

de Nooij, J. C., M. A. Letendre and I. K. Hariharan, 1996 A cyclin-dependent kinase inhibitor, Dacapo, is necessary for timely exit from the cell cycle during Drosophila embryogenesis. Cell **87:** 1237–1247.

de Nooij, J. C., K. H. Graber and I. K. Hariharan, 2000 Expression of the cyclin-dependent kinase inhibitor Dacapo is regulated by cyclin E. Mech. Dev. **97:** 73–83.

Dominguez, M., D. Ferres-Marco, F. J. Gutierrez-Avino, S. A. Speicher and M. Beneyto, 2004 Growth and specification of the eye are controlled independently by Eyegone and Eyeless in *Drosophila melanogaster*. Nat. Genet. **36:** 31–39.

Duman-Scheel, M., L. Weng, S. Xin and W. Du, 2002 Hedgehog regulates cell growth and proliferation by inducing Cyclin D and Cyclin E. Nature **417:** 299–304.

Firth, L. C., and N. E. Baker, 2005 Extracellular signals responsible for spatially regulated proliferation in the differentiating *Drosophila* eye. Dev. Cell **8:** 541–551.

Forbes, A. J., H. Lin, P. W. Ingham and A. C. Spradling, 1996 *hedgehog* is required for the proliferation and specification of ovarian somatic cells prior to egg chamber formation in Drosophila. Development **122:** 1125–1135.

Frankfort, B. J., and G. Mardon, 2002 R8 development in the *Drosophila* eye: a paradigm for neural selection and differentiation. Development **129:** 1295–1306.

Frankfort, B. J., R. Nolo, Z. Zhang, H. Bellen and G. Mardon, 2001 *senseless* repression of *rough* is required for R8 photoreceptor differentiation in the developing *Drosophila* eye. Neuron **32:** 403–414.

Freeman, M., 1997 Cell determination strategies in the *Drosophila* eye. Development **124:** 261–270.

Freemont, P. S., 2000 RING for destruction? Curr. Biol. **10:** R84–R87.

Fu, W., and N. E. Baker, 2003 Deciphering synergistic and redundant roles of Hedgehog, Decapentaplegic and Delta that drive the wave of differentiation in *Drosophila* eye development. Development **130:** 5229–5239.

Gao, S., M. M. Witte and R. E. Scott, 2002 P2P-R protein localizes to the nucleolus of interphase cells and the periphery of chromosomes in mitotic cells which show maximum P2P-R immunoreactivity. J. Cell Physiol. **191:** 145–154.

Gibson, M. C., and N. Perrimon, 2005 Extrusion and death of DPP/BMP-compromised epithelial cells in the developing *Drosophila* wing. Science **307:** 1785–1789.

Greenwood, S., and G. Struhl, 1999 Progression of the morphogenetic furrow in the *Drosophila* eye: the roles of Hedgehog, Decapentaplegic and the Raf pathway. Development **126:** 5795–5808.

Hay, B. A., T. Wolff and G. M. Rubin, 1994 Expression of baculovirus P35 prevents cell death in *Drosophila*. Development **120:** 2121–2129.

Heberlein, U., and K. Moses, 1995 Mechanisms of *Drosophila* retinal morphogenesis: the virtues of being progressive. Cell **81:** 987–990.

Higashijima, S.-I., T. Kojima, T. Michiue, S. Ishimaru, Y. Emori *et al.*, 1992 Dual *Bar* homeo box genes of *Drosophila* required in two photoreceptor cells, R1 and R6, and primary pigment cells for normal eye development. Genes Dev. **6:** 50–60.

Horsfield, J., A. Penton, J. Secombe, F. M. Hoffmann and H. Richardson, 1998 *decapentaplegic* is required for arrest in G1 phase during *Drosophila* eye development. Development **125:** 5069–5078.

Ives, P., 1950 New mutants report: bar-3. Dros. Inf. Serv. **24:** 58.

Jarman, A. P., Y. Grau, L. Y. Jan and Y. N. Jan, 1993 *atonal* is a proneural gene that directs chordotonal organ formation in the *Drosophila* peripheral nervous system. Cell **73:** 1307–1321.

Knoblich, J. A., and C. F. Lehner, 1993 Synergistic action of *Drosophila* cyclins A and B during the G2-M transition. EMBO J. **12:** 65–74.

Kumar, J. P., M. Tio, F. Hsiung, S. Akopyan, L. Gabay *et al.*, 1998 Dissecting the roles of the *Drosophila* EGF receptor in eye development and MAP kinase activation. Development **125:** 3875–3885.

Laski, F. A., and G. M. Rubin, 1989 Analysis of the *cis*-acting requirements for germ-line-specific splicing of the P-element ORF2–ORF3 intron. Genes Dev. **3:** 720–728.

Lee, J. J., D. P. von Kessler, S. Parks and P. A. Beachy, 1992 Secretion and localized transcription suggest a role in positional signaling for products of the segmentation gene *hedgehog*. Cell **71:** 33–50.

Lum, L., and P. A. Beachy, 2004 The Hedgehog response network: sensors, switches, and routers. Science **304:** 1755–1759.

Luo, L., T. Lee, L. Tsai, G. Tang, L. Y. Jan *et al.*, 1997 Genghis Khan (Gek) as a putative effector for *Drosophila* Cdc42 and regulator of actin polymerization. Proc. Natl. Acad. Sci. USA **94:** 12963–12968.

Ma, C., Y. Zhou, P. A. Beachy and K. Moses, 1993 The segment polarity gene *hedgehog* is required for progression of the morphogenetic furrow in the developing *Drosophila* eye. Cell **75:** 927–938.

Mason, J. M., and K. M. Arndt, 2004 Coiled coil domains: stability, specificity, and biological implications. Chembiochem **5:** 170–176.

Mohler, J., 1988 Requirements for *hedgehog*, a segmental polarity gene, in patterning larval and adult cuticle of Drosophila. Genetics **120:** 1061–1072.

Moses, K., M. C. Ellis and G. M. Rubin, 1989 The *glass* gene encodes a zinc-finger protein required by *Drosophila* photoreceptor cells. Nature **340:** 531–536.

Motzny, C. K., and R. Holmgren, 1995 The *Drosophila* cubitus interruptus protein and its role in the *wingless* and *hedgehog* signal transduction pathways. Mech. Dev. **52:** 137–150.

Myers, M., and M. McCullers, 1999 *Austin Powers: The Spy Who Shagged Me*. New Line Cinema, Los Angeles.

Nagaraj, R., and U. Banerjee, 2004 The little R cell that could. Int. J. Dev. Biol. **48:** 755–760.

Nagel, A. C., and A. Preiss, 1999 *Notch*^{spl} is deficient for inductive processes in the eye, and *E(spl)*^{D} enhances *split* by interfering with proneural activity. Dev. Biol. **208:** 406–415.

Newsome, T. P., B. Asling and B. J. Dickson, 2000 Analysis of *Drosophila* photoreceptor axon guidance in eye-specific mosaics. Development **127:** 851–860.

Nüsslein-Volhard, C., and E. Wieschaus, 1980 Mutations affecting segment number and polarity in *Drosophila*. Nature **287:** 795–801.

O'Neill, E. M., I. Rebay, R. Tjian and G. M. Rubin, 1994 The activities of two Ets-related transcription factors required for *Drosophila* eye development are modulated by the Ras/MAPK pathway. Cell **78:** 137–147.

Pagliarini, R. A., and T. Xu, 2003 A genetic screen in *Drosophila* for metastatic behavior. Science **302:** 1227–1231.

Penton, A., S. B. Selleck and F. M. Hoffmann, 1997 Regulation of cell cycle synchronization by *decapentaplegic* during *Drosophila* eye development. Science **275:** 203–206.

Persson, U., H. Izumi, S. Souchelnytskyi, S. Itoh, S. Grimsby *et al.*, 1998 The L45 loop in type I receptors for TGF-beta family members is a critical determinant in specifying Smad isoform activation. FEBS Lett. **434:** 83–87.

Pignoni, F., and S. L. Zipursky, 1997 Induction of *Drosophila* eye development by Decapentaplegic. Development **124:** 271–278.

Porter, J. A., D. P. von Kessler, S. C. Ekker, K. E. Young, J. J. Lee *et al.*, 1995 The product of Hedgehog autoproteolytic cleavage active in local and long-range signaling. Nature **374:** 363–366.

Ready, D. F., T. E. Hanson and S. Benzer, 1976 Development of the *Drosophila* retina, a neurocrystalline lattice. Dev. Biol. **53:** 217–240.

Richardson, H., L. V. O'Keefe, T. Marty and R. Saint, 1995 Ectopic cyclin E expression induces premature entry into S phase and disrupts pattern formation in the *Drosophila* eye imaginal disc. Development **121:** 3371–3379.

Roy, S., and P. W. Ingham, 2002 Hedgehogs tryst with the cell cycle. J. Cell Sci. **115:** 4393–4397.

Rubin, G. M., and A. C. Spradling, 1982 Genetic transformation of *Drosophila* with transposable element vectors. Science **218:** 348–353.

Sakai, Y., M. Saijo, K. Coelho, T. Kishino, N. Niikawa *et al.*, 1995 cDNA sequence and chromosomal localization of a novel human protein, RBQ-1 (RBBP6), that binds to the retinoblastoma gene product. Genomics **30:** 98–101.

Sambrook, J., E. F. Fritsch and T. Maniatis, 1989 *Molecular Cloning: A Laboratory Manual*. Cold Spring Harbor Laboratory Press, Cold Spring Harbor, NY.

Scott, R. E., and S. Gao, 2002 P2P-R deficiency modifies nocodazole-induced mitotic arrest and UV-induced apoptosis. Anticancer Res. **22:** 3837–3842.

Shen, J., and C. Dahmann, 2005 Extrusion of cells with inappropriate Dpp signaling from *Drosophila* wing disc epithelia. Science **307:** 1789–1790.

Simons, A., C. Melamed-Bessudo, R. Wolkowicz, J. Sperling, R. Sperling *et al.*, 1997 PACT: cloning and characterization of a cellular p53 binding protein that interacts with Rb. Oncogene **14:** 145–155.

Spradling, A. C., D. Stern, A. Beaton, E. J. Rhem, T. Laverty *et al.*, 1999 The Berkeley *Drosophila* Genome Project gene disruption project: single *P*-element insertions mutating 25% of vital Drosophila genes. Genetics **153:** 135–177.

Srinivasan, A., K. A. Roth, R. O. Sayers, K. S. Shindler, A. M. Wong *et al.*, 1998 *In situ* immunodetection of activated caspase-3 in apoptotic neurons in the developing nervous system. Cell Death Differ. **5:** 1004–1016.

Strutt, D. I., and M. Mlodzik, 1996 The regulation of *hedgehog* and *decapentaplegic* during *Drosophila* eye imaginal disc development. Mech. Dev. **58:** 39–50.

Summers, M. F., 1991 Zinc finger motif for single-stranded nucleic acids? Investigations by nuclear magnetic resonance. J. Cell Biochem. **45:** 41–48.

Tapon, N., N. Ito, B. J. Dickson, J. E. Treisman and I. K. Hariharan, 2001 The *Drosophila* tuberous sclerosis complex gene homologs restrict cell growth and cell proliferation. Cell **105:** 345–355.

Thomas, B. J., D. A. Gunning, J. Cho and S. L. Zipursky, 1994 Cell cycle progression in the developing *Drosophila* eye: *roughex* encodes a novel protein required for the establishment of G1. Cell **77:** 1003–1014.

Thummel, C. S., and V. Pirotta, 1992 Technical notes: new pCaSpeR P-element vectors. Dros. Inf. Serv. **71:** 150.

Tio, M., and K. Moses, 1997 The *Drosophila* TGFα homolog Spitz acts in photoreceptor recruitment in the developing retina. Development **124:** 343–351.

Tomlinson, A., 1985 The cellular dynamics of pattern formation in the eye of *Drosophila*. J. Embryol. Exp. Morphol. **89:** 313–331.

Tomlinson, A., 1988 Cellular interactions in the developing *Drosophila* eye. Development **104:** 183–193.

Treisman, J. E., and G. M. Rubin, 1995 *wingless* inhibits morphogenetic furrow movement in the *Drosophila* eye disc. Development **121:** 3519–3527.

Tseng, A. S., and I. K. Hariharan, 2002 An overexpression screen in Drosophila for genes that restrict growth or cell-cycle progression in the developing eye. Genetics **162:** 229–243.

Vo, L. T., M. Minet, J. M. Schmitter, F. Lacroute and F. Wyers, 2001 Mpe1, a zinc knuckle protein, is an essential component of yeast cleavage and polyadenylation factor required for the cleavage and polyadenylation of mRNA. Mol. Cell. Biol. **21:** 8346–8356.

Voas, M. G., and I. Rebay, 2004 Signal integration during development: insights from the *Drosophila* eye. Dev. Dyn. **229:** 162–175.

Wiersdorff, V., T. Lecuit, S. M. Cohen and M. Mlodzik, 1996 *Mad* acts downstream of Dpp receptors, revealing a differential requirement for *dpp* signaling in initiation and propagation of morphogenesis in the *Drosophila* eye. Development **122:** 2153–2162.

Witte, M. M., and R. E. Scott, 1997 The proliferation potential protein-related (P2P-R) gene with domains encoding heterogeneous nuclear ribonucleoprotein association and Rb1 binding shows repressed expression during terminal differentiation. Proc. Natl. Acad. Sci. USA **94:** 1212–1217.

Wolff, T., 2000 Histological techniques for the *Drosophila* eye part 1: larva and pupa, pp. 200–227 in *Drosophila Protocols*, edited by W. Sullivan, M. Ashburner and R. S. Hawley. Cold Spring Harbor Laboratory Press, Cold Spring Harbor, NY.

Wolff, T., and D. F. Ready, 1991 Cell death in normal and rough eye mutants of *Drosophila*. Development **113:** 825–839.

Xu, T., and G. M. Rubin, 1993 Analysis of genetic mosaics in developing and adult *Drosophila* tissues. Development **117:** 1223–1237.

Communicating editor: T. C. Kaufman